Comparative study of metal-cluster fission in Hartree-Fock and local-density approximations

Andrey Lyalin*
Institute of Physics, St. Petersburg State University, Ulianovskaja 1, St. Petersburg, Petrodvorez, Russia 198504

Andrey Solov'yov† and Walter Greiner
Institut für Theoretische Physik der Universität Frankfurt am Main, Robert-Mayer 8-10, Frankfurt am Main, Germany 60054
(Received 6 December 2001; published 5 April 2002)

Fission of doubly charged metal clusters is studied using the open-shell two-center deformed jellium Hartree-Fock model and local density approximation. Results of calculations of the electronic structure and fission barriers for the symmetric and asymmetric channels associated with the following processes $Na_{10}^{2+} \rightarrow Na_7^+ + Na_3^+$, $Na_{18}^{2+} \rightarrow Na_{15}^+ + Na_3^+$ and $Na_{18}^{2+} \rightarrow 2Na_9^+$ are presented. The role of the exact exchange and many-body correlation effects in metal clusters fission is analyzed. It is demonstrated that the influence of many-electron correlation effects on the height of the fission barrier is more profound if the barrier arises nearby or beyond the scission point. The importance of cluster deformation effects in the fission process is elucidated with the use of the overlapping-spheroids shape parametrization allowing one an independent variation of deformations in the parent and daughter clusters.

DOI: 10.1103/PhysRevA.65.043202 PACS number(s): 36.40.Qv, 31.10.+z, 31.15.Ne, 36.40.Wa

I. INTRODUCTION

Fission of charged atomic clusters occurs when repulsive Coulomb forces, arising due to the excessive charge, overcome the electronic binding energy of the cluster [1–3]. This mechanism of the cluster fission is in a great deal similar to the nuclear fission phenomena. Experimentally, multiply charged metal clusters can be observed in the mass spectra when their size exceeds the critical size of stability, which depends on the metal species and cluster charge [4–9]. For clusters above critical size, simple evaporation of neutral species is the dominant fragmentation channel, while below the critical size, fission into two charged fragments is more probable. At a low temperature fissioning clusters can be metastable above a certain size, because of the existence of a fission barrier.

Initially, theoretical studies of cluster stability were based on pure energetic criteria that only involved the energies of the initial and the final states [10–12]. Later, a simple one-center liquid drop model (LDM), which was initially suggested by Lord Rayleigh in 1882 [13] and later widely used in nuclear physics, was adapted to charged metal clusters [14]. In this model, one introduces the ''fissility parameter,'' $X = E_{Coul}^{shere}/2E_{Surf}^{sphere}$, which is proportional to the ratio of the Coulomb to surface energy of charged spherical liquid drop [13]. The fissility parameter distinguishes the situations when cluster is unstable, metastable, or stable. The investigation of the Rayleigh instabilities in multiply charged sodium clusters has been done in Ref. [15], where reasonable agreement with experimental data was found.

In spite of the fact that the simple LDM qualitatively describes the fission process it fails to reproduce experimental data in full detail. This happens because the LDM does not take into account shell effects. It has been shown that the shell effects are important in nuclear fission [18] and even more important in fission of metal clusters [7]. One can describe the shell effects in metal clusters using the shell correction method, originally developed in nuclear physics [16–18]. This method was adapted for metal clusters in Refs. [19–24].

The asymmetric two-center-oscillator shell model (ATCOSM), introduced in Ref. [25] for nuclear fission is quite successful in prediction of the fission barriers. This model was also applied for the description of metal-cluster fission [26]. Although ATCOSM method uses single electron model potential it has the significant advantage in comparison to other models allowing one simple shape parametrization and an independent variation of deformations in the parent and daughter clusters [26].

The microscopic description of energetics and dynamics of metal-cluster fission process based on molecular-dynamic (MD) simulations has been performed in Refs. [27–30] using the local-spin-density-functional method. This method is, however, strongly restricted by the cluster size, because of computational difficulties, and thus is usually applied to the small metal clusters with the number of atoms $N \leqslant 20$.

Fission process of metal clusters can be also simulated on the basis of the jellium model, which does not take into account the detailed ionic structure of the cluster core. Jellium model considers the electrons in the usual quantum-mechanical way, but approximates the cluster core potential by the potential of the homogeneous positively charged background and, therefore, is better applicable for lager cluster sizes (see, e.g., [31] for review). Most of the electronic structure calculations of the jellium metal clusters have been performed using self-consistent Kohn-Sham local density approximation (LDA) [32]. The LDA jellium calculations for metal-cluster fission can be grouped [26] into two categories according to the fragment shape parametrization, namely, the

*Email address: lyalin@rpro.ioffe.rssi.ru
†Permanent address: A. F. Ioffe Physical-Technical Institute of the Russian Academy of Sciences, Polytechnicheskaya 26, St. Petersburg, Russia 194021; Email address: solovyov@rpro.ioffe.rssi.ru

 ©2002 The American Physical Society

two-intersected-spheres jellium [33–35] and variable-necking-in parametrization [36–38]. It has been shown that the cluster shape parametrization must be flexible enough to account for the majority of effects generated by the shell structure of the parent and daughter clusters, which in general have not spherical but deformed shapes [26].

The important feature of the LDA method consists in the fact that it takes into account many-electron correlations via the phenomenological exchange-correlation potential (see, e.g., [39,40] for review). However, so far, there has not been found the unique potential, universally applicable for different systems and conditions. As a result there is a ''zoo of potentials'' [41] valid for special cases. These potentials, of course, do exist, in principle, as unique quantities but are not actually understood, so they cannot serve as a satisfactory basis for achieving a physical interpretation.

Alternatively, one can develop direct *ab initio* methods for the description of electronic properties of metal clusters. It can be achieved by using the Hartree-Fock (HF) approximation and by the construction on its basis the systematic many-body theories such as the random-phase approximation with exchange [42], many-body perturbation theory or the Dyson equation method [43–45]. Based on fundamental physical principles these models can be refined by extending the quality of the approximations, while the physical meaning of the effects included are clearly demonstrated and thus give more accurate characteristics of metal clusters than LDA.

Originally, the Hartree-Fock model for the metal-cluster electron structure has been worked out in the framework of spherically symmetric jellium approximation in Refs. [46,47]. It is valid for the clusters with closed electronic shells that correspond to magic numbers (8, 20, 34, 40, . . .). On the basis of the Hartree-Fock approach the dynamic jellium model has been proposed [48,49]. This model treats simultaneously the vibrational modes of the ionic jellium background, the quantized electron motion and the interaction between the electronic and the ionic subsystems. In particular, the dynamic jellium model allows to describe the widths of electron excitations in metal clusters beyond the adiabatic approximation. The open-shell two-center jellium Hartree-Fock approximation valid for metal clusters with arbitrary number of the valence electrons has been developed in Refs. [50,51]. The two-center jellium HF method treats the quantized electron motion in the field of the spheroidal ionic jellium background in the spheroidal coordinates. This method has been generalized and adopted to study the metal-clusters fission process in our recent work [52], where barrier for the symmetric fission cannel $Na_{18}{}^{2+} \rightarrow 2Na_9{}^{+}$ was calculated.

In the present work we investigate the role of the exchange and correlation effects in metal-cluster fission process on the basis of both the Hartree-Fock and LDA methods. Both symmetric and asymmetric fission channels for the $Na_{10}{}^{2+}$ and $Na_{18}{}^{2+}$ parent clusters are considered. Comparison of results of the two approaches allows us to illustrate the importance of the exchange component of the many-electron interaction in the fission process and make important conclusion about the relative role of the two different channels of the reaction.

The atomic system of units, $|e|=m_e=\hbar=1$, has been used throughout the paper, unless other units not indicated.

II. THEORETICAL METHODS

A. Two-center jellium model and cluster shape parametrization

According to the main postulate of the jellium model, the electron motion in a metallic cluster takes place in the field of the uniform positive charge distribution of the ionic background. For the parametrization of the ionic background during the fission process we consider the model in which the initial parent cluster having the form of the ellipsoid of revolution (spheroid) splits into two independently deformed spheroids of smaller size [52]. The two principal diameters a_k and b_k of the spheroids can be expressed via the deformation parameter δ_k as

$$a_k=\left(\frac{2+\delta_k}{2-\delta_k}\right)^{2/3}R_k,\quad b_k=\left(\frac{2-\delta_k}{2+\delta_k}\right)^{1/3}R_k. \tag{2.1}$$

Here partial indexes $k=0,1,2$ correspond to the parent cluster ($k=0$) and the two daughter fragments ($k=1,2$), R_k ($k=0,1,2$) are the radii of the corresponding undeformed spherical cluster. The deformation parameters δ_k characterize the families of the prolate ($\delta_k>0$) and the oblate ($\delta_k<0$) spheroids of equal volume $V_k=4\pi a_k b_k^2/3=4\pi R_k^3/3$.

The radii of the parent and the resulting nonoverlapping daughter fragments are equal to $R_k=r_s N_k^{1/3}$, where N_k is the number of atoms in the kth cluster, and r_s is the Wigner-Seitz radius. For sodium clusters, $r_s=4.0$, which corresponds to the density of the bulk sodium. For overlapping region the radii $R_1(d)$ and $R_2(d)$ are functions of the distance d between the centers of mass of the two fragments. They are so determined that the total volume inside the two spheroids equals the volume of the parent cluster $4\pi R_0^3/3$.

The ions charge density $\rho(\mathbf{r})$ is kept uniform including the overlapping-spheroids region,

$$\rho(\mathbf{r})=\begin{cases}\rho_c & (x^2+y^2)/b_1^2+(z+d/2)^2/a_1^2\leqslant 1\\ \rho_c & (x^2+y^2)/b_2^2+(z-d/2)^2/a_2^2\leqslant 1\\ 0 & \text{otherwise.}\end{cases} \tag{2.2}$$

Here $\rho_c=Z_0/V_0$ is the ionic charge density inside the cluster and Z_0 is the total charge of the ionic core.

The electrostatic potential $U_{core}(\mathbf{r})$ of the ionic background can be determined from the solution of the corresponding Poisson equation

$$\Delta U_{core}(\mathbf{r})=-4\pi\rho(\mathbf{r}). \tag{2.3}$$

B. Hartree-Fock and LDA formalism

The Hartree-Fock equations can be written out explicitly in the form (see, e.g., [53]):

$$(-\Delta/2+U_{core}+U_{HF})|a\rangle=\varepsilon_a|a\rangle. \tag{2.4}$$

The first term here represents the kinetic energy of electron a, and U_{core} its attraction to the cluster core. The Hartree-Fock potential U_{HF} represents the average Coulomb interaction of electron a with the other electrons in the cluster, including the nonlocal exchange interaction, and ε_a describes the single-electron energy.

According to the density-functional theory, the ground-state energy is a minimum for the exact density of the functional of the density of the system [54]. A self-consistent method for calculation of the electronic states of many-electron systems was proposed by Kohn and Sham [32]. This method leads to the Kohn-Sham LDA self-consistent equations, which are similar to the Hartree equations

$$(-\Delta/2+U_{core}+U_H+V_{xc})|a\rangle=\varepsilon_a|a\rangle. \tag{2.5}$$

Here U_H is the Hartree potential, which represents the direct Coulomb interaction of electron a with the other electrons in the cluster, but does not take into account the nonlocal exchange effects, while V_{xc} is the phenomenological density dependent local exchange-correlation potential. In the present work we use the Gunnarsson and Lundqvist model [55] for the LDA electron exchange-correlation energy density ϵ_{xc}, which reads as

$$\epsilon_{xc}(\rho_{el}(\mathbf{r}))=-\frac{3}{4}\left(\frac{9}{4\pi^2}\right)^{1/3}\frac{1}{r_s(\mathbf{r})}-0.0333G(r_s(\mathbf{r})/11.4). \tag{2.6}$$

Here $r_s(\mathbf{r})=[3/4\pi\rho_{el}(\mathbf{r})]^{1/3}$ is a *local* Wigner-Seitz radius, while $\rho_{el}(\mathbf{r})$ is the electron density in the cluster, and the function $G(x)$ is defined by following relation:

$$G(x)=(1+x^3)\ln\left(1+\frac{1}{x}\right)-x^2+\frac{x}{2}-\frac{1}{3}. \tag{2.7}$$

The exchange-correlation energy density $\epsilon_{xc}(\rho_{el}(\mathbf{r}))$, defines the LDA exchange-correlation potential $V_{xc}(\rho_{el}(\mathbf{r}))$ as

$$\begin{aligned}V_{xc}(\rho_{el}(\mathbf{r}))&=\frac{\delta(\rho_{el}(\mathbf{r})\epsilon_{xc}(\rho_{el}(\mathbf{r})))}{\delta\rho_{el}(\mathbf{r})}\\&=-\left(\frac{9}{4\pi^2}\right)^{1/3}\frac{1}{r_s(\mathbf{r})}\\&\quad-0.0333\ln\left(1+\frac{11.4}{r_s(\mathbf{r})}\right).\end{aligned} \tag{2.8}$$

The Hartree-Fock (2.4) and LDA (2.5) equations have been solved in the system of the prolate spheroidal coordinates as a system of coupled two-dimensional second-order partial differential equations. The partial differential equations have been discretized on a two-dimensional grid and the resulting system of linear equations has been solved numerically by the successive overrelaxation method [56]. This technique is different from that we have used in our previous works [50–52], where the expansion of wave functions and potentials over spheroidal harmonics in the prolate and oblate spheroidal coordinates in one dimension and a numerical expansion for the second dimension have been carried out. The third dimension, the azimuthal angle, has been treated analytically in both methods. Our calculations show that the partial-expansion method is effective for slightly deformed systems, for which only few terms in the expansion are necessary to take into account in order to achieve sufficient accuracy. However, for strongly deformed systems, or process like fission, the direct two-dimensional integration is more efficient.

The important characteristic of the cluster, which defines its stability is the total energy E_{tot}. The total energy of the cluster is equal to the sum of the electrostatic energy of the ionic core E_{core} and the energy of the valence electrons E_{el}

$$E_{tot}=E_{core}+E_{el}. \tag{2.9}$$

The electrostatic energy of the cluster ionic core is equal to

$$E_{core}=\frac{1}{2}\int_V\rho(\mathbf{r})U_{core}(\mathbf{r})\mathrm{d}\mathbf{r}. \tag{2.10}$$

In the Hartree-Fock approximation, the electronic energy E_{el} is given by the general expression [53]

$$\begin{aligned}E_{el}^{HF}&=\sum_a\langle a|-\Delta/2+U_{core}|a\rangle\\&\quad+\frac{1}{2}\sum_{abk}q_aq_b[c(abk)F^k(a,b)+d(abk)G^k(a,b)],\end{aligned} \tag{2.11}$$

where a and b run over all shells. The values $F^k(a,b)$ and $G^k(a,b)$ in the Eq. (2.11) are the Coulomb and exchange Slater integrals, q_a and q_b are the occupation numbers for orbitals a and b, respectively. The Hatree-Fock coefficients $c(abk)$ and $d(abk)$ for the Coulomb and exchange energy contributions depend on the occupation numbers (see for details [53]).

In the framework of LDA the electronic energy of the system is given by [32,54]

$$\begin{aligned}E_{el}^{LDA}&=\sum_a\langle a|-\Delta/2+U_{core}|a\rangle+\frac{1}{2}\int\frac{\rho_{el}(\mathbf{r})\rho_{el}(\mathbf{r}')}{|\mathbf{r}-\mathbf{r}'|}\,\mathrm{d}\mathbf{r}\mathrm{d}\mathbf{r}'\\&\quad+\int\rho_{el}(\mathbf{r})\epsilon_{xc}(\rho_{el}(\mathbf{r}))\mathrm{d}\mathbf{r},\end{aligned} \tag{2.12}$$

where the latter term represents the exchange-correlation energy.

III. NUMERICAL RESULTS

Let us present and discuss the results of calculations performed in the model described above. We start our consideration with the analysis of electronic configurations and occupation numbers alterations during the fission processes of the doubly charged sodium clusters Na_{10}^{2+} and Na_{18}^{2+}, which we perform using the two overlapping sphere parametriza-

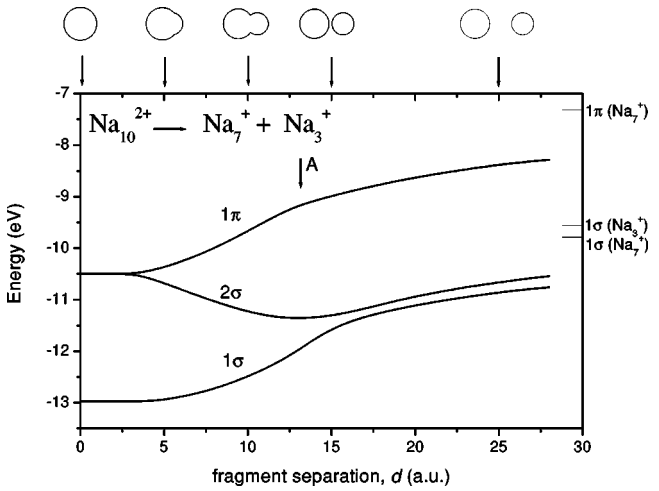

FIG. 1. Hartree-Fock single-electron energy levels for the asymmetric fission channel $Na_{10}^{2+} \rightarrow Na_7^+ + Na_3^+$ as a function of fragments separation distance d, when both the parent and daughter clusters are spherical ($\delta_0 = \delta_1 = \delta_2 = 0$). The evolution of the cluster shape during the fission process is shown on top of the figure. Horizontal lines on the right-hand side of the figure mark the Hartree-Fock energy levels for the free daughter fragments.

tion model. The second part of our discussion is devoted to the cluster energetics and formation of fission barriers, for the fission channels considered. We compare the results obtained for the two overlapping spheres and the two overlapping-spheroids parametrization, as well as the variable-necking-in type of the shape parametrization and demonstrate the crucial importance of the cluster shape deformations in the fission process.

Figures 1–3 show the Hartree-Fock single-electron energies ε_i as a function of the fragment separation distance d for the following asymmetric $Na_{10}^{2+} \rightarrow Na_7^+ + Na_3^+$, $Na_{18}^{2+} \rightarrow Na_{15}^+ + Na_3^+$ and symmetric $Na_{18}^{2+} \rightarrow 2Na_9^+$ channels, respectively, when both parent and daughter clusters are assumed to be spherical, and, hence, for any d the deformation

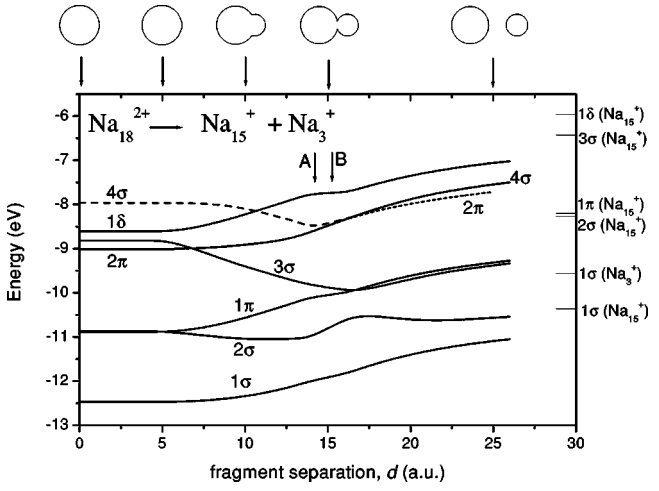

FIG. 2. The same as Fig. 1 but for asymmetric fission channel $Na_{18}^{2+} \rightarrow Na_{15}^+ + Na_3^+$. Lowest unoccupied states are shown by dashed (4σ) and short dashed (1δ) lines.

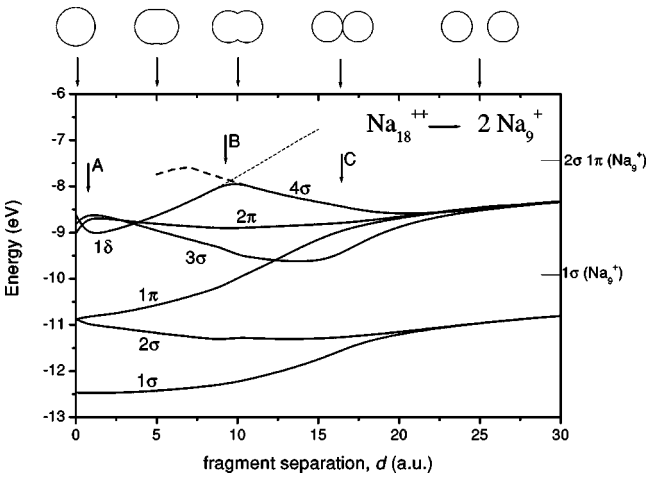

FIG. 3. The same as Fig. 1 but for symmetric fission channel $Na_{18}^{2+} \rightarrow 2Na_9^+$. Lowest unoccupied states are shown by dashed (4σ) and short dashed (2π) lines.

parameters are equal to zero $\delta_0 = \delta_1 = \delta_2 = 0$. The snapshots of the cluster shape evolution during the fission are shown on top of each figure.

The initial electronic configuration for the parent Na_{10}^{2+} cluster is $1\sigma^2 2\sigma^2 1\pi^4$, where $2\sigma 1\pi$ level is degenerated, due to spherical symmetry of the system with closed electronic shells. With increasing fragments separation distance d, the spherical symmetry of the parent cluster breaks down, that results in splitting of the single-electron energy levels according to projection of the angular momentum along the z axis. A similar splitting of the energy levels has been studied for deformed nuclei (see, e.g., [57]) and clusters [50,51]. For high enough separation distances beyond the scission point, indicated by vertical arrow A in Fig. 1, energy levels approach to their limiting values marked by horizontal lines on the right-hand side of the figure, being the electron energy levels of the free fission fragments Na_7^+ ($1\sigma^2 1\pi^4$) and Na_3^+ ($1\sigma^2$).

The electronic configuration and the orbital occupation numbers for Na_{18}^{2+} cluster exhibits several alterations during the fission process, as it is shown in Fig. 2 and 3. This happens due to the fact that different electronic configurations minimize the total energy of the cluster at different separation distances. The parent cluster Na_{18}^{2+} has the initial electronic configuration $1\sigma^2 2\sigma^2 1\pi^4 2\pi^2 3\sigma^2 1\delta^4$. Following the asymmetric channel of fission $Na_{18}^{2+} \rightarrow Na_{15}^+ + Na_3^+$ (see Fig. 2) the new configuration $1\sigma^2 2\sigma^2 1\pi^4 3\sigma^2 4\sigma^2 1\delta^4$ becomes preferable, when two electrons transfer from the half-filled 2π state to initially unoccupied 4σ state. This happens for the separation distance $d \geqslant 14.2$ a.u. (marked in Fig. 2 by the solid vertical arrow A) before the scission point (vertical arrow B) $d = 15.3$ a.u. The order of the energy levels manifests several redistributions during the fission process, and finally for high enough separation distance ($d > 25$ a.u.), its energy levels correspond to the free fission fragments Na_{15}^+ ($1\sigma^2 2\sigma^2 1\pi^4 3\sigma^2 1\delta^4$) and Na_3^+ ($1\sigma^2$).

For the symmetric fission channel $Na_{18}^{2+} \rightarrow 2Na_9^+$ (Fig. 3) the energy levels show even more complicated behavior. Thus, for the separation distance $d \geqslant 0.7$ a.u. (marked

in Fig. 3 by solid vertical arrow *A*) the new intermediate configuration $1\sigma^2 2\sigma^2 1\pi^4 1\delta^2 2\pi^4 3\sigma^2$ becomes preferable, when two electrons transfer from the occupied 1δ to the half-filled 2π state. Further increasing of the separation distance, leads to the transition of the two residual 1δ electrons to the initially unoccupied 4σ state for $d \geqslant 9.25$ a.u. (marked in Fig. 3 by the solid vertical arrow *B*) forming the final electronic configuration $1\sigma^2 2\sigma^2 1\pi^4 3\sigma^2 2\pi^4 4\sigma^2$ before the scission point (vertical arrow *C*) $d=16.64$ a.u. The order of the energy levels manifests several redistributions during the fission process, and finally for high enough separation distance ($d>25$ a.u.), its ordering corresponds to $1\sigma 2\sigma 1\pi$ that determined by the magic spherical Na_9^+ products. They are doubly degenerated as compared to the initial configuration, since there are two Na_9^+ fragments in the system. Such a behavior of the HF levels as a function of *d* is quite similar to those following from the ATCOSM simulations [26].

Figure 4 presents fission barriers for the asymmetric channel $Na_{10}^{2+} \rightarrow Na_7^+ + Na_3^+$ as a function of the fragments separation distance *d*. In order to perform the accurate comparison of fission barriers derived in the two-center deformed jellium HF and LDA models with the ATCOSM results [26], we have used two different types of shape parametrization. Thus, the upper part in Fig. 4 shows the barriers for fission of a spherical parent cluster into two spherical daughter fragments (i.e., $\delta_0=\delta_1=\delta_2=0$ in our model). This type of parametrization, known as the two-intersected spheres parametrization, was used in many works [33–35]. The low part in Fig. 4 shows fission barriers derived on the basis of parametrization accounting for an independent deformation of parent and daughter clusters in order to minimize the total energy of the system for any distance *d*. The evolution of cluster shape during the fission process is shown for the HF and LDA models on tops of the corresponding figures. Note, that the variable-necking-in parametrization has been used in the ATCOSM calculation [26].

Solid lines in Fig. 4 are the result of the two-center jellium HF model, while dashed curves have been calculated in LDA. Dash-dotted lines show the ATCOSM barriers calculated in Ref. [26]. The zero of energy put at $d=0$.

Figure 4(a) demonstrates a good agreement of the HF and ATCOSM fission barriers heights $\Delta_{HF}=\Delta_{ATCOSM}=0.95$ eV. The LDA value for the fission barrier, $\Delta_{LDA}=1.30$ eV, slightly exceeds the HF and ATCOSM ones. In HF and LDA schemes the fission barrier maximum is located just behind the scission point (marked by vertical arrow *A*).

The two-intersected spheres parametrization is not adequate for the description of the process $Na_{10}^{2+} \rightarrow Na_7^+ + Na_3^+$, because Na_7^+ daughter fragment has an open-shell electronic structure, and, therefore, its shape is not spherical because it undergoes Jahn-Teller distortion [24]. The deformed jellium Hartree-Fock and LDA calculations show that the ground state of the Na_7^+ cluster has the oblate shape with the deformation parameter $\delta_1=-0.68$. This value is in a good agreement with other theoretical estimates [50]. The oblate shape deformation of the daughter cluster reduces the final total energy of the system E_{tot} by -1.32 eV for the HF, and by -1.05 eV for the LDA model calculations, in comparison with the spherical case.

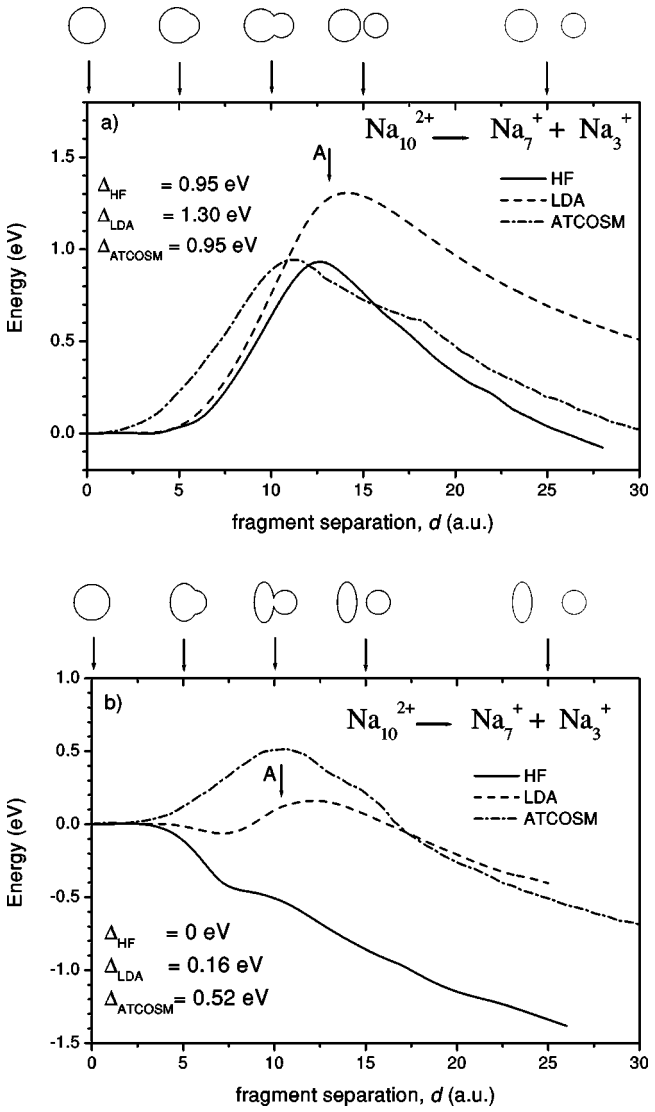

FIG. 4. Fission barriers in the two-center deformed jellium Hartree-Fock (solid lines) and LDA (dashed lines) approaches calculated in this work for the asymmetric channel $Na_{10}^{2+} \rightarrow Na_7^+ + Na_3^+$ as a function of fragments separation distance *d*. In (a), both parent and daughter clusters are spherical, $\delta_0=\delta_1=\delta_2=0$. In (b), deformations of the parent and daughter clusters are taken into account. The zero of energy put at $d=0$. The evolution of cluster shape during the fission process is shown on top of (a) and (b) for both models. We compare our results with those derived in ATCOSM (dash-dotted line) [26].

Figure 4(b) shows fission barriers for the asymmetric channel $Na_{10}^{2+} \rightarrow Na_7^+ + Na_3^+$, when spheroidal deformations of the parent and daughter clusters are taken into account. We have minimized the total energy of the system over the parent and daughter fragments deformations with the aim to find the fission pathway corresponding to the minimum of the fission barrier. We have also used the assumption of continuous shape deformation during the fission process. The deformation of the cluster fragments changes drastically the fission energetics in comparison with what follows from the two-intersected spheres model. In the framework of the two-center deformed jellium Hartree-Fock

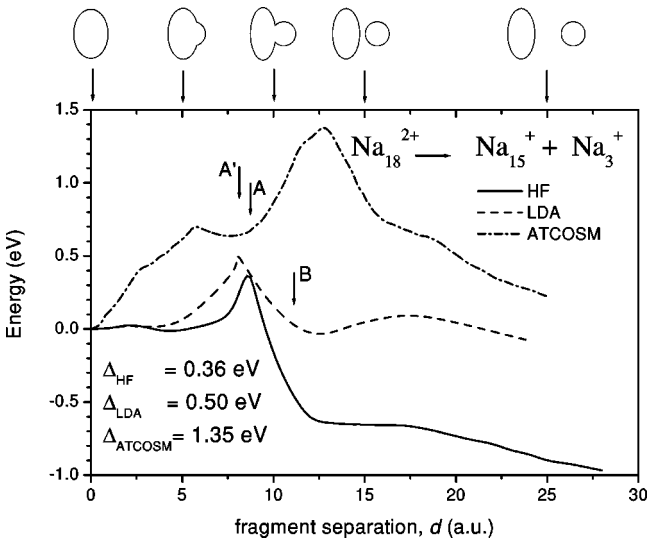

FIG. 5. The same as Fig. 4, but for the asymmetric channel $Na_{18}^{2+} \rightarrow Na_{15}^{+} + Na_3^{+}$.

approximation, the parent cluster Na_{10}^{2+} becomes unstable towards the asymmetric channel $Na_{10}^{2+} \rightarrow Na_7^{+} + Na_3^{+}$.

The LDA simulations with deformation of the daughter fission fragments take into account the decrease of the total energy of the system [see Fig. 4(b)]. In particular, this results in the appearance of the local minimum in the energy curve at $d=7.2$ a.u., corresponding to the formation of the superdeformed asymmetric prolate shape of the parent Na_{10}^{2+} cluster before the scission point *A*. The latter is located at $d=10.4$ a.u. The allowance for deformation of the parent cluster and the fission fragments reduces the LDA fission barrier up to the value $\Delta_{LDA}=0.16$ eV, which is in rather poor agreement with the result of ATCOSM $\Delta_{ATCOSM}=0.52$ eV.

It is necessary to note that the shape of the cluster fragments in ATCOSM has been parametrized by two spheroids of revolution connected by a smooth neck [26]. Our calculations show that the oblate shape of Na_7^{+} fragment is formed at the initial stage of fission process, for separation distances before the scission point. Moreover, in the vicinity of the scission point, where the interaction between the two daughter fragments Na_7^{+} and Na_3^{+} is strong, the oblate Na_7^{+} fragment is even more deformed than a free one. This means that it is more favorable for two fragments to split at shorter distances rather than to be connected by a smooth neck, making the system more prolate. This fact explains why using of necking-type of shape parametrization, leads to the higher barrier as compare to our parametrization.

Comparison of the asymmetric $Na_{18}^{2+} \rightarrow Na_{15}^{+} + Na_3^{+}$ and symmetric $Na_{18}^{2+} \rightarrow 2Na_9^{+}$ fission channels of the parent Na_{18}^{2+} cluster is a subject of particular interest, because there have to be a competition between these two channels involving magic cluster-ions Na_3^{+} and Na_9^{+}. In Refs. [6,23,27] it was noticed that, namely, in fission of the Na_{18}^{2+} cluster a magic fragment other than Na_3^{+} becomes the favored channel. Fig. 5 shows fission barriers for the asymmetric channel $Na_{18}^{2+} \rightarrow Na_{15}^{+} + Na_3^{+}$. We have started from the initial configuration corresponding to oblate shape of the parent Na_{18}^{2+} cluster with the deformation parameter $\delta_0 = -0.35$. The oblate deformation reduces the total energy of the cluster Na_{18}^{2+} by -0.58 eV for the HF and by -0.48 eV for the LDA model in comparison with the spherical case. We have minimized the total energy of the system over the deformation parameters of the parent and daughter fragments during the fission process for any separation distance *d*. The evolution of the fragment shapes is shown on top of the figure for both HF and LDA models. The daughter fragment Na_{15}^{+} has an oblate shape with deformation parameter $\delta_1 = -0.6$, while Na_3^{+} is spherical, i.e., $\delta_2 = 0$.

The total energy as a function of the fragment separation distance has a maximum (marked by vertical arrow *A* for HF, and A' for LDA), arising due to the alteration of the electronic configuration $1\sigma^2 2\sigma^2 1\pi^4 2\pi^2 3\sigma^2 1\delta^4 \rightarrow 1\sigma^2 2\sigma^2 1\pi^4 3\sigma^2 4\sigma^2 1\delta^4$. These maxima on the energy curves define the fission barrier heights, being equal to $\Delta_{HF}=0.36$ eV for Hartree-Fock and $\Delta_{LDA}=0.50$ eV for LDA. It is interesting to notice that the LDA total energy curve has a pronounced minimum at $d=12.5$ a.u., located beyond the scission point $d=11.1$ a.u. We have marked the scission point by vertical arrow *B*, both for HF and LDA. This minimum means that a quasistable state of the supermolecule $Na_{15}^{+} + Na_3^{+}$ can be created during the fission process. However, the appearance of the minimum and thus the stability of the supermolecule is rather sensitive to the model chosen for the description of exchange and correlation interelectron interaction. This is already clear from the fact that such a minimum does not appear in the HF simulations (see Fig. 5).

The ATCOSM model calculation gives the value of the fission barrier $\Delta_{ATCOSM}=1.35$ eV, which is inconsistent with the HF and LDA results derived in our model. Such a difference can be explained as a result of variable necking in type of the shape parametrization, which has been used in Ref. [26]. In the case of asymmetric $Na_{18}^{2+} \rightarrow Na_{15}^{+} + Na_3^{+}$ channel, the parent as well as one of the daughter fragments have an oblate shape, therefore, shape parametrization model with prolatelike additional neck is not natural, and results in increasing the fission barrier.

Figure 6 shows the dependence of total energy E_{tot} on separation distance *d* for the symmetric channel $Na_{18}^{2+} \rightarrow 2Na_9^{+}$. The parent cluster changes its shape from oblate to prolate one on the initial stage of the fission process ($d \approx 1$ a.u.). This transition is accompanied by the first rearrangement of the electronic configuration (marked by vertical arrow *A* for HF and A' for LDA). This process has the barrier $\Delta_{HF}=0.63$ eV and $\Delta_{LDA}=0.48$ eV. On the next stage of the reaction the prolate deformation develops resulting in the highly deformed cluster shape, as it is shown on top of Fig. 6. At the distance $d \approx 11$ (marked by vertical arrow *B* for HF, and B' for LDA) the electronic configuration reaches its final form being the same as in the spherical Na_9^{+} products. In this case, the variable necking in type of fragments shape parametrization used in ATCOSM does not break the symmetry of the fragments and, therefore, the agreement between the two overlapped-spheroids HF or LDA models and ATCOSM variable-necking-in approach is much better than

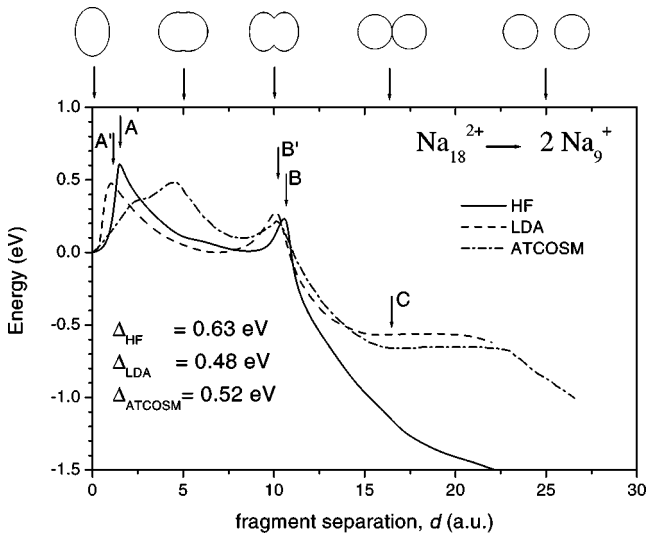

FIG. 6. The same as Fig. 4, but for the symmetric channel $Na_{18}^{2+} \rightarrow 2Na_9^+$

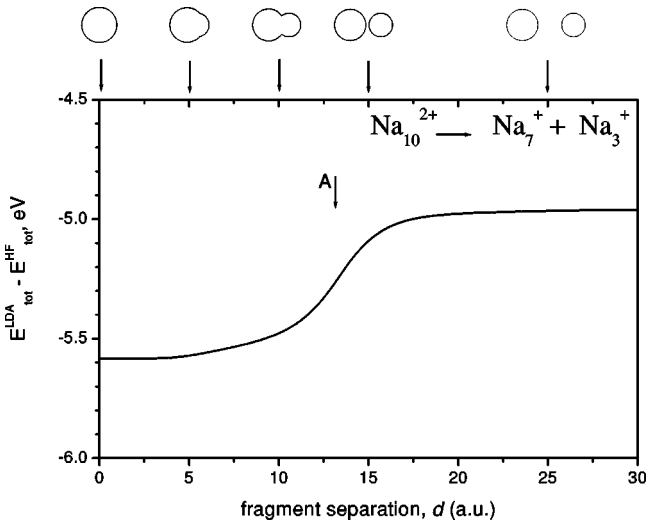

FIG. 7. Difference between the LDA and HF total energies as a function of fragments separation distance for the fission channel $Na_{10}^{2+} \rightarrow Na_7^+ + Na_3^+$. The evolution of the cluster shape during the fission process is shown on top of the figure. Vertical arrow *A* corresponds to the scission point.

in the case of asymmetric fission channel. Indeed, the total fission barrier for the symmetric channel $Na_{18}^{2+} \rightarrow 2Na_9^+$ is equal to $\Delta_{HF}=0.63$ eV and $\Delta_{LDA}=0.48$ eV in the two-center jellium Hartree-Fock and LDA models, respectively. These values are in a good agreement with the ATCOSM result $\Delta_{ATCOSM}=0.52$ eV [26].

In Table I we have summarized the results of the HF and LDA barrier heights calculations for the considered fission channels and compared them with the results of ATCOSM [26] and MD simulations [27,29,30].

The height of the fission barrier for Na_{10}^{2+} cluster in the two-center deformed jellium LDA model is 0.51 eV lower than its value following from the MD simulations [29]. Molecular-dynamics simulations performed in Ref. [29] also were based on the density-functional theory, but included full ionic structure of the cluster. Since both methods apply the same form of the density functional [55], the discrepancy in the fission barrier heights can be attributed to the manifestation of the influence of the cluster ionic structure in the fission process. One can expect that the influence of the detailed ionic structure has to decrease with the growth cluster size, making the jellium model approach more and more accurate. However, we also want to notice here that different schemes of MD simulations [27,29,30] lead to somewhat different fission barrier heights (see Table I).

For the Na_{18}^{2+} cluster, we report a very good agreement of the heights of fission barriers derived in the jellium LDA model and MD [29]. It is interesting to note that MD simulations predict the asymmetric channel $Na_{18}^{2+} \rightarrow Na_{15}^+ + Na_3^+$ to be a little more favorable, however, the jellium LDA model says in favor of the symmetric path $Na_{18}^{2+} \rightarrow 2Na_9^+$. Although, in both models the difference in the heights of symmetric and asymmetric fission barriers is rather small, being equal to 0.02 eV.

Finally, let us compare the results obtained in the HF and LDA models. The Hartree-Fock model takes into account the exchange interelectron interaction the most exactly, but it neglects many-electron correlations, playing quite a significant role in metal-cluster energetics. Thus, LDA calculations with the Gunnarsson-Lundqvist's exchange-correlation potential [55] lower the total energy E_{tot} of the parent Na_{10}^{2+} and Na_{18}^{2+} clusters on -5.58 eV and -12.03 eV, respectively, as compared to the energies calculated in the Hartree-Fock approximation. Such a difference between the total energies of the HF and LDA jellium clusters is a result of the manifestation of many-electron correlation interaction. The many-electron correlation interaction reduces at distances *d* beyond the scission point, when the parent cluster splits on the two fragments, due to decrease of the number of interacting electrons in the system.

Figure 7 shows the difference between the LDA and HF total cluster energies $E_{tot}^{LDA}-E_{tot}^{HF}$ as a function of fragments separation distance for the fission channel $Na_{10}^{2+} \rightarrow Na_7^+ + Na_3^+$. For illustrative purposes we use here the two over-

TABLE I. Summary of the fission barrier heights in (eV) calculated in this work and their comparison with the results of other approaches.

Channel	HF	LDA	ATCOSM [26]	MD [29]	MD [30]	MD [27]
$Na_{10}^{2+} \rightarrow Na_7^+ + Na_3^+$	0	0.16	0.52	0.67	0.50	0.71
$Na_{18}^{2+} \rightarrow Na_{15}^+ + Na_3^+$	0.36	0.50	1.35	0.50		
$Na_{18}^{2+} \rightarrow 2Na_9^+$	0.63	0.48	0.52	0.52		

lapping sphere parametrization to dismiss the effect of the clusters fragment shape alteration along the fission pathway, which can be different in the HF or LDA schemes of calculation.

It is seen from Fig. 7 that the difference between the LDA and HF total energies $E_{tot}^{LDA}-E_{tot}^{HF}$ does not change significantly for separation distances below the scission point, in spite of the strong deformation of the parent cluster. In the narrow region of d, nearby the scission point the value $E_{tot}^{LDA}-E_{tot}^{HF}$ increases and it becomes constant again above the scission point. Such a behavior is in a great deal similar, at least qualitatively, to the all considered fission channels. It remains valid even if deformations of the parent and daughter fragments are taken into account. This fact has a simple physical explanation. The many-electron correlations reduce the total energy. During the fission process the many-electron correlation interaction between electrons belonging the two different cluster fragments vanishes, which results in the increase of the total energy of the system.

In spite of the fact that many-electron correlations reduce significantly the total energy of the $Na_{10}{}^{2+}$ and $Na_{18}{}^{2+}$ jellium clusters in comparison with the HF values, the difference in heights of the fission barriers obtained in the HF and LDA models is only about 0.15 eV. From the analysis carried out above one can conclude that many-electron correlations do not influence significantly on the height of the fission barrier if the latter arises well below before the scission point. In the cases when the barrier is created nearby or above the scission point, accounting for many-electron correlations becomes essential. For example, many-electron correlations play the crucial role for the $Na_{10}{}^{2+}\rightarrow Na_7{}^{+}+Na_3{}^{+}$ fission channel. In this case the HF model predicts qualitatively wrong barrierless scenario of the fission. In the contrary, the agreement between the HF and LDA models is much better for both symmetric and asymmetric fission channels of the $Na_{18}{}^{2+}$ cluster. Note also that the HF model, predicts the asymmetric fission channel $Na_{18}{}^{2+}\rightarrow Na_{15}{}^{+}+Na_3{}^{+}$ to be more favorable in comparison with the symmetric one.

IV. SUMMARY

We have developed the open-shell two-center deformed jellium Hartree-Fock and LDA method for the description of metal-clusters fission process. The proposed two overlapping-spheroids shape parametrization allows one to consider independently a wide variety of shape deformations of parent and daughter clusters, and to investigate the role of deformation effects on the cluster fission process. The proposed type of shape parametrization is preferable as compared to variable-necking-in one, in particular, when the fission fragments have an oblate shape. The role of many-electron correlation effects in metal-clusters fission is analyzed. The described Hartree-Fock model forms the basis for further systematic development of the more advanced *ab initio* many-body theories for the process of metal-clusters fission.

ACKNOWLEDGMENTS

The authors acknowledge financial support from the Volkswagen Foundation, the Alexander von Humboldt Foundation, INTAS, DFG, DAAD, and the Royal Society of London.

[1] K. Sattler, J. Mühlbach, O. Echt, P. Pfau, and E. Recknagel, Phys. Rev. Lett. **47**, 160 (1981).
[2] U. Näher, S. Bjornholm, F. Frauendorf, and C. Guet, Phys. Rep. **285**, 245 (1997).
[3] C. Yannouleas, U. Landman, and R. N. Barnett, in *Metal Clusters*, edited by W. Ekardt (Wiley, New York, 1999), p. 145.
[4] C. Bréchignac, Ph. Cahuzac, F. Carlier, and J. Leygnier, Phys. Rev. Lett. **63**, 1368 (1989).
[5] C. Bréchignac, Ph. Cahuzac, F. Carlier, and M. de Frutos Phys. Rev. Lett. **64**, 2893 (1990).
[6] C. Bréchignac, Ph. Cahuzac, F. Carlier, J. Leygnier, and A. Sarfati, Phys. Rev. B **44**, 11 386 (1991).
[7] C. Bréchignac, Ph. Cahuzac, F. Carlier, and M. de Frutos, Phys. Rev. B **49**, 2825 (1994).
[8] T.P. Martin, J. Chem. Phys. **81**, 4426 (1984).
[9] T.P. Martin, U. Nähler, H. Göhlich, and T. Lange, Chem. Phys. Lett. **196**, 113 (1992).
[10] D. Tomanek, S. Mukerjee, and K.H. Bennemann, Phys. Rev. B **28**, 665 (1983).
[11] M.P. Iñiguez, J.A. Alonso, M.A. Aller, and L.C. Balbás, Phys. Rev. B **34**, 2152 (1986).
[12] B.K. Rao, P. Jena, M. Manninen, and R.M. Mieminen, Phys. Rev. Lett. **58**, 1188 (1987).
[13] Lord Rayleigh, Philos. Mag. **14**, 185 (1882).
[14] W.A. Saunders, Phys. Rev. A **46**, 7028 (1992).
[15] F. Chandezon, S. Tomita, D. Cormier, P. Grübling, C. Guet, H. Lebius, A. Pesnelle, and B.A. Huber, Phys. Rev. Lett. **87**, 153402 (2001).
[16] V.M. Strutinsky, Nucl. Phys. A **95**, 420 (1967).
[17] V.M. Strutinsky, Nucl. Phys. A **122**, 1 (1968).
[18] J.M. Eisenberg and W. Greiner, *Nuclear Theory* (North-Holland, Amsterdam, 1985).
[19] M. Nakamura, Y. Ishii, A. Tamura, and S. Sugano, Phys. Rev. A **42**, 2267 (1990).
[20] C. Yannouleas and U. Landman, Chem. Phys. Lett. **210**, 437 (1993).
[21] S.M. Reimann, M. Brack, and K. Hansen, Z. Phys. D: At., Mol. Clusters **28**, 235 (1993).
[22] H. Koizumi, S. Sugano, and Y. Ishi, Z. Phys. D: At., Mol. Clusters **28**, 223 (1993).
[23] C. Yannouleas and U. Landman, Phys. Rev. B **51**, 1902 (1995).
[24] S. Frauendorf and V.V. Pashkevich, Ann. Phys. (Leipzig) **5**, 34 (1996).
[25] J. Maruhn and W. Greiner, Z. Phys. **251**, 431 (1972).
[26] C. Yannouleas and U. Landman, J. Phys. Chem. **99**, 14 577 (1995).

[27] R.N. Barnett, U. Landman, and G. Rajagopal, Phys. Rev. Lett. **67**, 3058 (1991).
[28] C. Bréchignac, Ph. Cahuzac, F. Carlier, M. de Frutos, R.N. Barnett, and U. Landman, Phys. Rev. Lett. **72**, 1636 (1994).
[29] B. Montag and P.-G. Reinhard, Phys. Rev. B **52**, 16 365 (1995).
[30] P. Blaise, S.A. Blundell, C. Guet, and R.R. Zopa, Phys. Rev. Lett. **87**, 063401 (2001).
[31] W. Ekard, W.D. Schöne, and J.M. Pacheco, in *Metal Clusters*, edited by W. Ekardt (Wiley, New York, 1999), p. 1.
[32] W. Kohn and L.J. Sham, Phys. Rev. A **140**, 1133 (1965).
[33] S. Saito and S. Ohnishi, Phys. Rev. Lett. **59**, 190 (1987).
[34] S. Saito and M.L. Cohen, Phys. Rev. B **38**, 1123 (1988).
[35] E. Engel, U.R. Schmitt, H.-J. Lüdde, A. Toepfer, E. Wüst, R.M. Dreizler, O. Knospe, R. Schmidt, and P. Chattopadhyay, Phys. Rev. B **48**, 1862 (1993).
[36] F. Garcias, J.A. Alonso, M. Barranco, J.M. Lópes, A. Mañanes, and J. Németh, Z. Phys. D: At., Mol. Clusters **31**, 275 (1994).
[37] F. Garcias, A. Mañanes, J.M. Lópes, J.A. Alonso, and M. Barranco, Phys. Rev. B **51**, 1897 (1995).
[38] H. Koizumi and S. Sugano, Phys. Rev. A **51**, R886 (1995).
[39] R.G. Parr and W. Yang, *Density-Functional Theory of Atoms and Molecules* (Oxford University Press, Oxford, 1989).
[40] P. Fulde, *Electron Correlations in Molecules and Solids* (Springer-Verlag, Berlin, 1995).
[41] D. Salahub, *Atomic Clusters and Nanoparticles*, les Houches summer school, session LXXIII, les Houches, France, 2000, edited by C. Guet, P. Hobza, F. Spiegelman, and F. David (EDP Sciences, Springer-Verlag, Berlin, 2001).
[42] M. Ya. Amusia, *Atomic Photoeffect*, edited by P.G. Burke and H. Kleinpoppen (Plenum, New York, 1990).
[43] L.V. Chernysheva, G.F. Gribakin, V.K. Ivanov, and M.Yu. Kuchiev, J. Phys. B **21**, L419 (1988).
[44] G.F. Gribakin, B. Gul'tsev, V.K. Ivanov, and M.Yu. Kuchiev, J. Phys. B **23**, 4505 (1990).
[45] V.K. Ivanov, in *Correlations in Clusters and Related Systems*, edited by J.-P. Connerade (Worls Scientific, Singapore, 1996), pp. 73–91.
[46] C. Guet and W.R. Johnson, Phys. Rev. B **45**, 11 283 (1992).
[47] V.K. Ivanov, A.N. Ipatov, V.A. Kharchenko, and M.L. Zhizhin, Phys. Rev. A **50**, 1459 (1994).
[48] L.G. Gerchikov, A.V. Solov'yov, and W. Greiner, Int. J. Mod. Phys. E **8**, 289 (1999).
[49] L.G. Gerchikov, A.N. Ipatov, A.V. Solov'yov, and W. Greiner, J. Phys. B **44**, 4905 (2000).
[50] A.G. Lyalin, S.K. Semenov, A.V. Solov'yov, N.A. Cherepkov, and W. Greiner, J. Phys. B **33**, 3653 (2000)
[51] A.G. Lyalin, S.K. Semenov, A.V. Solov'yov, N.A. Cherepkov, J.-P. Connerade, and W. Greiner, J. Chin. Chem. Soc. (Taipei) **48**, 101 (2001).
[52] A.G. Lyalin, A.V. Solov'yov, W. Greiner, and S.K. Semenov, Phys. Rev. A **33**, 3653 (2000).
[53] I. Lindgren and J. Morrison, *Atomic Many-Body Theory* (Springer-Verlag, New York, 1986).
[54] P. Hohenberg and W. Kohn, Phys. Rev. **136**, 864 (1964).
[55] O. Gunnarsson and B.I. Lundqvist, Phys. Rev. B **13**, 4274 (1976).
[56] D.M. Young, *Iterative Solution of Large Linear Systems* (Academic Press, New York, 1971).
[57] A.B. Migdal, *Qualitative Methods of Quantum Mechanics* (Nauka, Moscow, 1978).